Magnetic properties of single-crystal $DyAl_2$

A. L. Lima,[1,*] A. O. Tsokol,[1] K. A. Gschneidner, Jr.,[1,2] V. K. Pecharsky,[1,2] T. A. Lograsso,[1] and D. L. Schlagel[1]
[1]*Materials and Engineering Physics Program, Ames Laboratory, Iowa State University, Ames, Iowa 50011-3020, USA*
[2]*Department of Materials Science and Engineering, Iowa State University, Ames, Iowa 50011-2300, USA*
(Received 10 January 2005; revised manuscript received 31 March 2005; published 1 July 2005)

We measured the magnetic properties and heat capacity of three $DyAl_2$ single crystals with the magnetic field oriented along the three principal crystallographic directions: [100], [110], and [111]. The isothermal entropy change versus temperature curves were obtained from heat capacity and magnetization data for these directions. The experimental results were successfully explained by a mean field model that includes spin reorientation, exchange interactions, and crystalline electric field effects. The anomalous magnetocaloric effect along the [111] direction predicted by theory was confirmed experimentally.

DOI: 10.1103/PhysRevB.72.024403 PACS number(s): 75.30.Sg, 71.20.Lp, 74.25.Ha, 75.10.Dg

INTRODUCTION

The search for advanced magnetic refrigerant materials has been on the forefront of condensed matter science over the last few years, since the discovery of giant magnetocaloric effect (GMCE) materials,[1] thus causing a new momentum towards the development of near room temperature magnetic cooling/heating technology and bringing the magnetic refrigeration closer to reality. The present effort is mostly concentrated on materials that have a large magnetocaloric effect (MCE) near room temperature such as $Gd_5(Si_{1-x}Ge_x)_4$,[1,2] $La(Fe_{1-x}Si_x)_{13}$,[3] $La(Fe_{1-x}Si_x)_{13}H_y$,[4] MnAs,[5] $MnFeP_{1-x}As_x$,[6] and a variety of manganites[7] The discovery of the GMCE also renewed interest in intermetallic compounds, which have been revisited over the last few years in order to evaluate their magnetocaloric properties. The two thermodynamic signatures of the magnetocaloric effect are the isothermal magnetic entropy change (ΔS_M) and the adiabatic temperature change (ΔT_{ad}) that are observed upon changes in the external magnetic field.

The rare earth intermetallic compounds have been in the spotlight because of their importance in basic research as well as for a variety of practical applications. The magnetic properties of the rare-earth intermetallics result, to a large extent, from the interplay between the crystalline electric field effects (CEFs) and the exchange interactions. The CEF removes the degeneracy of the ground multiplet of the rare earth ion, which may lead to specific features of the magnetic properties such as an anomalous magnetocaloric effect.[8] Theoretical studies are also in progress in order to understand and to predict magnetic properties of new materials.

As it is well known, all magnetic materials exhibit the magnetocaloric effect; for instance, for ferromagnetic materials with nearly zero coercivity and hysteresis, the magnetocaloric effect is observed as a peak in the ΔS_M vs. T curve or in the ΔT_{ad} vs. T curve at (or near) the Curie temperature (T_C).[9] However, the special features that lead to the GMCE are not yet well determined. In materials similar to $Gd_5(Si_{1-x}Ge_x)_4$,[1,2] the presence of a structural transition also plays an important role. Mainly in those cases where a structural transition is present, it is necessary to evaluate the magnetoelastic energy involved. The presence of magnetoelastic effects must also be taken into account in more detailed calculations of the MCE in conventional ferromagnetic systems.

The intermetallic compound $DyAl_2$ was found to have good magnetocaloric properties at low temperatures. This compound has been extensively studied both theoretically and experimentally.[8,10–13] At low temperature, the easy magnetization axis is the [100] direction, which changes to the [111] direction at ~40 K in zero magnetic field[10–12] or in an applied field of 57 kOe at 4 K.[10] A recent theoretical analysis[8] indicates that $DyAl_2$ should exhibit an anomaly in its ΔS_M vs. T curve, i.e., a negative MCE along the [111] direction below ~50 K. The anomaly was said to be associated with the change in the easy magnetization direction from the [100] to the [111]. As reported by Levin *et al.*,[14] the ac magnetic susceptibility of the polycrystalline $DyAl_2$ exhibits an anomaly at 42 K. In general, ac-susceptibility measurements are quite sensitive to detecting magnetic phase transitions initiated by a change of the magnetocrystalline anisotropy energy. It is expected that any spin reconfiguration, domain walls displacement, or magnetic anisotropy can be detected by measuring the ac susceptibility. The influence of spin reorientation on the magnetocaloric properties of this compound is, however, not completely clear.

In this paper, we present the results of an investigation of the magnetic and magnetocaloric properties of a $DyAl_2$ single crystal, which was cut into five smaller crystals (two for heat capacity studies and three for magnetization measurements) such that the applied magnetic field was parallel to three main crystallographic directions: [100], [110], and [111]. For the magnetization measurements, we had a single crystal for each direction, but for the heat capacity study we only had the [100] and [110] crystals. An attempt was made to prepare a $DyAl_2$ single crystal with the [111] orientation for the heat capacity measurements, but we were unable to cut one out of the master single crystal which was a pure [111] single crystal large enough for the heat capacity study. Experimental data are based on heat capacity data, which were measured from 3.5 to 350 K in several applied fields from 0 to 100 kOe, and magnetization data, which were measured isothermally as a function of field from 0 to 50 kOe for several temperatures between 5 and 110 K. From both the magnetization and the heat capacity data we computed the $\Delta S(T)_H$ functions, which were compared to theoretical results. Moreover, we measured the magnetic ac susceptibility in order to verify some of our results. As

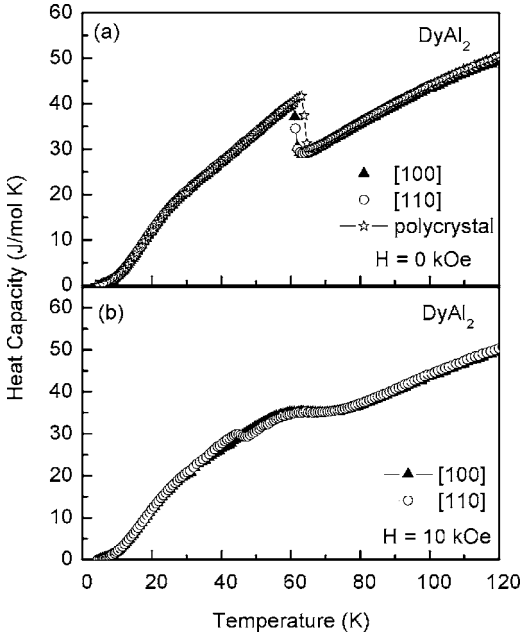

FIG. 1. (a) Comparison between the heat capacity of the two single crystals oriented in two of the three main crystallographic direction (open circles: [100], full triangles: [110]) and the polycrystal $DyAl_2$ (open stars). Note, the T_C of the polycrystalline sample is ~4 K higher than those of the single-crystal samples (see text). (b) The heat capacity for $DyAl_2$ with magnetic field vector parallel to either of the two main crystallographic directions (as noted in the figure) as a function of the temperature for an applied field of 10 kOe (open circles: [100], full triangles: [110]).

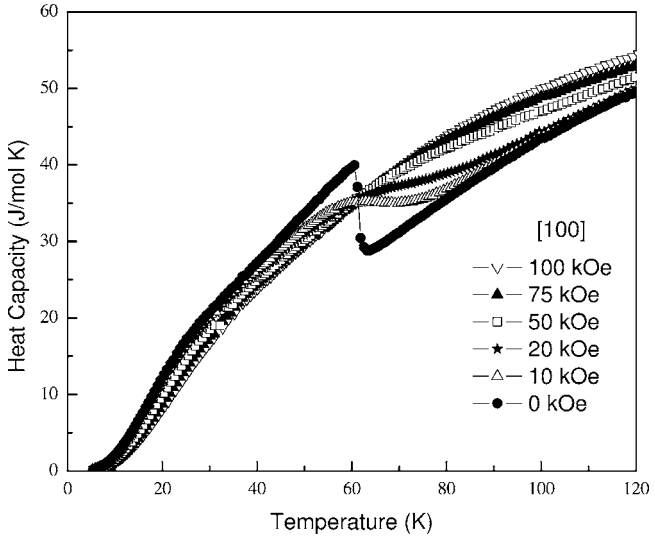

FIG. 2. The heat capacity of single-crystal $DyAl_2$ oriented for [100] parallel to the magnetic field vector as a function of the temperature for a zero field (full circles) and of applied fields of 10 kOe (open up triangles), 20 kOe (full stars), 50 kOe (open squares), 75 kOe (full triangles), and 100 K (open down triangles).

shown below, the results are fully understood by using a mean field theory that includes CEF effects, exchange interactions, and the Zeeman effect.

THEORY

The compound $DyAl_2$ crystallizes in the $MgCu_2$-type Laves phase structure. The point symmetry for the rare earth ion is $\bar{4}3m$, and, thus, the following Hamiltonian can be used to describe a system of magnetic rare earth (lanthanide) ions:

$$\hat{H} = \hat{H}_{CEF} + \hat{H}_{MAG}, \tag{1}$$

where

$$\hat{H}_{CEF} = W\left[\frac{X}{F_4}(O_4^0 + 5O_4^4) + \frac{(1-|X|)}{F_6}(O_6^0 - 21O_6^4)\right], \tag{2a}$$

which can be written as

$$\hat{H}_{CEF} = [B_4(O_4^0 + 5O_4^4) + B_6(O_6^0 - 21O_6^4)] \tag{2b}$$

and

$$\hat{H}_{MAG} = -g\mu_B B[J^x \cos(\alpha) + J^y \cos(\beta) + J^z \cos(\gamma)]. \tag{3}$$

Equation (2a) represents the CEF interaction for an ion in Lea-Leask-Wolf notation,[15] where W is the energy scale of CEF and is equal to −0.019 eV, while X $(-1<X<1)$ gives the relative importance between the contribution of the fourth- and sixth-order Stevens operators, O_n^m [Eq. (2b)]. B_4 and B_6 are functions of the parameter X while F_4 and F_6 are dimensionless constants: $F_4=60$ and $F_6=13862$.[15] Equation (3) describes the Zeeman effect, and B, the effective magnetic field experienced by the system, is given by the molecular field approximation:

$$B_m^n = B_0 \cos(\phi) + \lambda M^n \quad \text{for } n = x,y,z \text{ and } \phi = \alpha,\beta,\gamma, \tag{4}$$

where B_0 is the applied field, M^n is the magnetization calculated using an extended Bak model,[10,16] and λ is the exchange parameter. The cosines are the direction cosines for the three main directions in the crystal. The CEF parameters B_4 and B_6 were taken from Purwins and Leson,[10] i.e., $B_4 = -(5.5\pm1.2)\times10^{-5}$ meV and $B_6 = -(5.6\pm0.8)\times10^{-7}$ meV. These values were used to calculate MCE along the [100] and [110] directions, but for the [111] direction B_4 was reduced about 0.4% to -5.52×10^{-5} meV in order to get agreement between the observed and calculated T_C. This slight change in the B_4 parameter is well within the error limits of the values given by Purwins and Leson. One of the most important aspects of writing the effective field as in Eq. (4) is the freedom to apply the external field B_0 in any direction, and not necessarily in any of the main directions. Moreover, the system can be allowed to rotate so that the spin reorientation can be included.

Once the Hamiltonian is solved self-consistenly, the ε_i eigenvalues and $|\varepsilon_i\rangle$ eigenstates are used to obtain the partition function from which the magnetic properties are calculated. It is worth noting that the magnetization is dependent on the temperature so that the Hamiltonian is temperature dependent for the self-consistent procedure in this model. For the total entropy evaluation, we need to include, besides the magnetic contribution, the lattice and electronic entro-

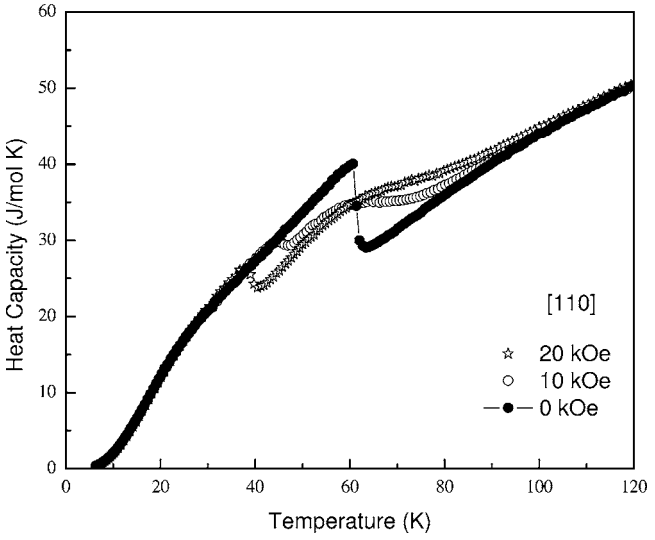

FIG. 3. The heat capacity of single-crystal $DyAl_2$ oriented for [110] parallel to the magnetic field vector as a function of the temperature for a zero field (full circles) and applied fields of 10 kOe (open circles) and 20 kOe (full stars).

pies. The lattice entropy was determined by prorating the lattice entropies of the nonmagnetic extremes of the lanthanide series (La and Lu) according to the following relation:

$$S_{lattice}^{DyAl_2}(T) = \left(\frac{9 \times S_{lattice}^{LuAl_2} + 5 \times S_{lattice}^{LaAl_2}}{14} \right). \quad (5)$$

Since both the electronic and lattice contributions may be considered magnetic field independent, the change of the entropy of the system at a given temperature[17] can be described by

$$-\Delta S_M(T,B_0) = S(T,B_0=0) - S(T,B_0) = S_M(T,B_0=0) - S_M(T,B_0). \quad (6)$$

The theoretical ΔS_M can be compared to the one obtained experimentally using Eq. (6) with the total entropies determined from the heat capacity

$$C_{p,B} = T\left(\frac{\partial S}{\partial T}\right)_{p,B}, \quad (7)$$

or from the bulk magnetization data using Maxwell's relation:

$$\left(\frac{\partial S_M}{\partial B}\right)_T = \left(\frac{\partial M}{\partial T}\right)_B. \quad (8)$$

EXPERIMENTAL DETAILS

A $DyAl_2$ single crystal was grown using the Bridgman technique from a polycrystalline material of the same stoichiometry, which was arc melted using 99.8 at. % pure Dy (the major impurties were the interstitial elements O and C) and 99.999 at. % Al. The as-grown crystal was oriented using the backscattered Laue technique. Two different specimens in the form of parallelepipeds (approximate dimensions $10\times10\times3$ mm^3) with the largest face of each crystal parallel to [100] and [110] planes were employed for the heat capacity measurements using an adiabatic heat pulse calorimeter.[18] Similarly, three different specimens in forms of parallelepipeds (approximate dimensions $2\times2\times5$ mm^3) with the [100], [110], and [111] directions normal to one of the faces of each parallelepiped were employed in the magnetization and magnetic susceptibility measurements using a Lake Shore magnetometer. The combined accuracy of the alignment of the magnetic field vector with a specific crystallographic direction in both the calorimeter and magnetometer is estimated to be ±5°.

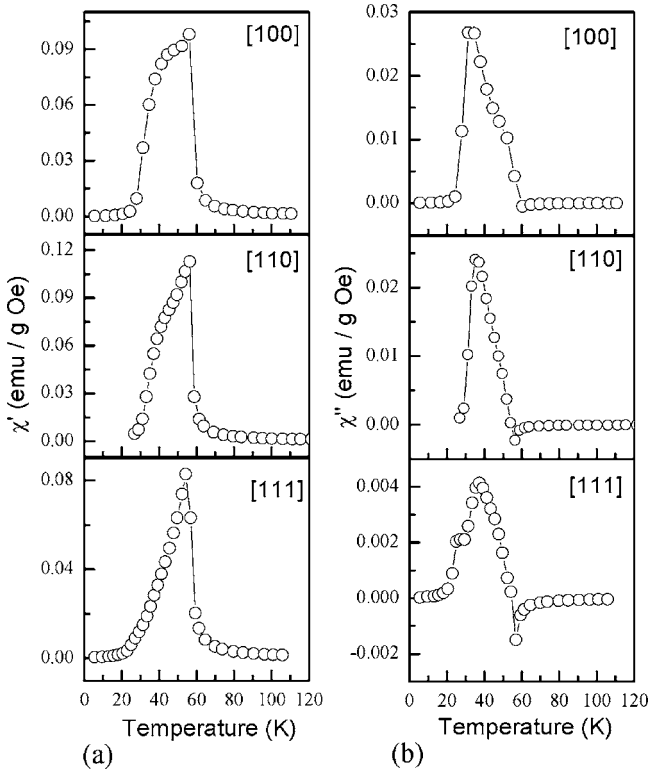

FIG. 4. (a) The real part of the ac susceptibility as a function of the temperature for $H_{dc}=0$ Oe, $H_{ac}=5$ Oe, and $f=125$ Hz of three $DyAl_2$ single crystals aligned with the ac field vector collinear with the three principle crystallographic axes. (b) The imaginary part of the ac susceptibility as a function of the temperature for $H_{dc}=0$ Oe, $H_{ac}=5$ Oe, and $F=125$ Hz of three $DyAl_2$ single crystals aligned with the ac field vector collinear with the three principle crystallographic axes.

RESULTS AND DISCUSSION

Figure 1(a) shows the heat capacity as a function of temperature for zero magnetic field from 3.5 to 120 K for the two single crystals oriented such that either the [100] or the [110] crystallographic directions are parallel to the magnetic field vector. Also shown for comparison are the polycrystal data. As expected, in the absence of the magnetic field, there is no anisotropy and all of the heat capacity curves are the same. However, the T_C of the polycrystalline sample is slightly higher (~4 K) than that of the single crystals. This

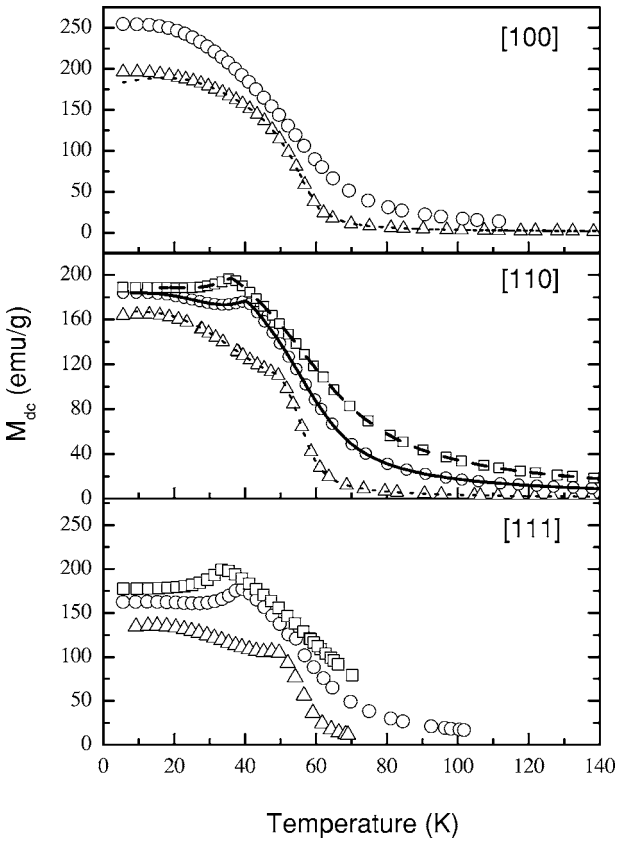

FIG. 5. The magnetization curves as a function of the temperature for the three single crystals. For the [100] direction, open up triangles: $H=2$ kOe, heating, ZFC; dotted line: $H=2$ kOe, cooling; open circles: $H=10$ kOe, heating, ZFC. For the [110] direction, open up triangles: $H=2$ kOe, heating, ZFC; dotted line: $H=2$ kOe, cooling; open circles: $H=10$ kOe, heating, ZFC; continuous line: $H=10$ kOe, cooling; open squares: $H=20$ kOe, heating, ZFC; dashed line: $H=20$ kOe, cooling. For the [111] direction, open up triangles: $H=2$ kOe, heating, ZFC; open circles: $H=10$ kOe, heating, ZFC; open squares: $H=20$ kOe, heating, ZFC.

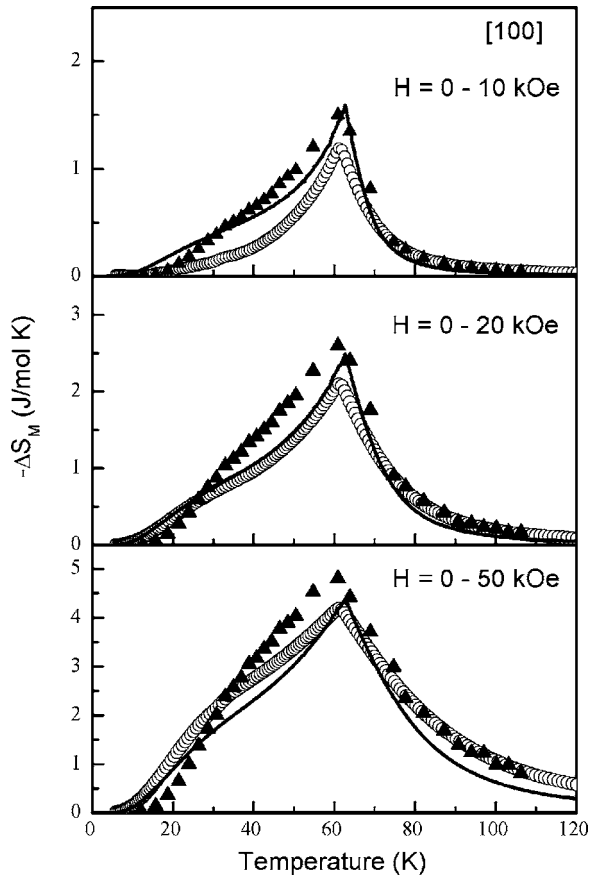

FIG. 6. Comparison between the isothermal entropy change calculated (continuous line) and that obtained from experimental data extracted from heat capacity (open dots) and extracted from magnetization (full triangles) for the $DyAl_2$ single crystal aligned along the [100] direction.

may be due to small changes in the chemical composition of the polycrystalline sample relative to that of the single crystal. When a magnetic field is applied [see Fig. 1(b)] the behaviors of the heat capacities of the single crystals change significantly. This becomes more obvious when one compares the low magnetic field heat capacity results shown in Figs. 2 and 3. The $H=10$ kOe and 20 kOe curves for [110] direction exhibit a bump near 40 K (Fig. 3), unlike that for [100] direction (Fig. 2). For higher applied fields, the anomaly vanishes and the anisotropy of the samples no longer exists and the heat capacity curves with magnetic fields of 50 kOe and higher lie on top of one another regardless of the orientation of a crystal with respect to the field vector.

Both the real χ'_{ac} [Fig. 4(a)] and the imaginary χ''_{ac} [Fig. 4(b)] components of the ac magnetic susceptibility were measured as a function of tempreature from ~5 to 120 K. Their behavior reflects the magnetization and its dynamics in a material as a function of temperature. The real component of the ac susceptibility is the initial susceptibility in phase with the applied ac field and it is correlated with the reversible initial magnetization process. From χ'_{ac} it is possible to evaluate how difficult it is to initiate the magnetization of the material. On the other hand, χ''_{ac} is related to the irreversible magnetization process that is observed in the hysteresis loop. It gives an estimate of the energy loss during the initial magnetization process and it represents the susceptibility having a $\pi/2$ phase shift with respect to the applied field. All three orientations exhibit a peak at ~55 K [Fig. 4(a)] which is slightly lower than the Curie temperatures observed in the heat capacity (see Figs. 1–3). This slight difference in Curie temperatures from the two different measurements is consistent with the variation of Curie temperatures reported in literature for the various types of measurements.[10] For the [100] and [110] single crystals, the amplitudes and the shapes of the χ'_{ac} curves are somewhat similar and they resemble that of polycrystalline $DyAl_2$ (Ref. 14) with a slight bump at ~35 K which is due to the spin reorientation process. For the imaginary part, a peak is observed for all three single-crystal samples near the 35 K spin reorientation temperature with the onset at the Curie temprature (~58 K). For the [111] direction, a broad two-step peak is apparent, instead of a sharp peak observed for the other two directions. The fact that χ''_{ac} is not zero between 20 and 60 K in all of the directions is a confirmation that domain walls movements are present.

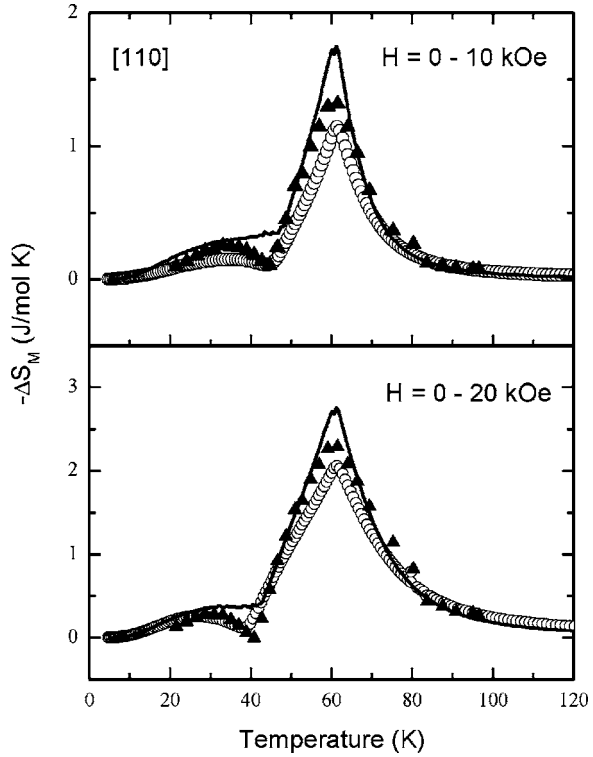

FIG. 7. Comparison between the isothermal entropy change calculated (continuous line) and that obtained from experimental data extracted from heat capacity (open dots) and extracted from magnetization (full triangles) for the $DyAl_2$ single crystal aligned along the [110] direction.

The magnetization as function of the temperature for the [100], [110], and [111] directions is presented in Fig. 5. These data confirmed that the [100] direction is the easy magnetization direction at 5 K. When the magnetic field was applied parallel to the [100] direction, the magnetization in a 10 kOe field shows no anomalies that can be related to spin reorientation. On the contrary, for the [111] and [110] directions, the peaks observed near 35 K are related to the spin reorientation and the temperatures are in agreement with literature.[10–12] The magnetization curves for [111] and [110] are similar in shape and in absolute value, although the curve for [110] has slightly higher saturation values. The saturation value for [100] is significantly larger than in [110] and [111]. It is worthwhile to note that for the [110] direction, the magnetization curve also exhibits a small decrease just below the peak in the 10 kOe magnetization curve, which is primarily due to the rotation of the magnetization from [100] to [111].

Figures 6–8 show a comparison between the isothermal entropy change calculated from theory and the experimental values obtained from the magnetization and heat capacity measurements (except in Fig. 8 where only the magnetization results are shown). The theoretical curves agree quite well with the experimental ΔS_M values. For the [100] direction (Fig. 6) the MCE curves are quite smooth and do not show any unusual features. For the [110] direction (see Fig. 7) the low-temperature broad-peak, observed at 25 K, is due to the spin reorientation.

The most interesting MCE, however, is observed in the ΔS_M vs. T curve for the [111] direction [Fig. 8(a)]. In this

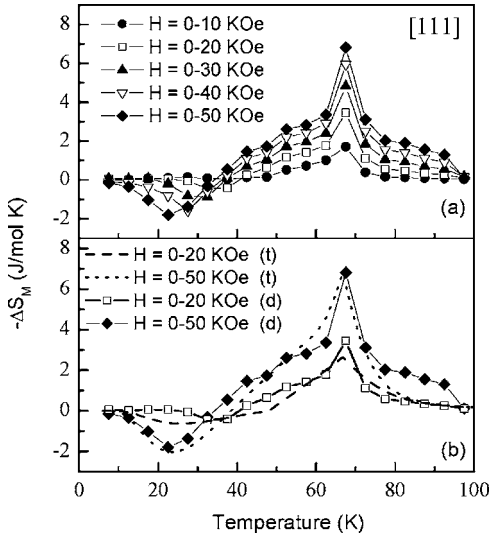

FIG. 8. (a) The isothermal entropy change obtained from experimental data extracted from the magnetization for the $DyAl_2$ single crystal aligned along the [111] direction. (b) A comparison of the theoretical MCE (dotted and dashed lines) with the experimental (data points) results for the same conditions as in (a). The continuous lines connecting the data points are guides for the eye.

case, a negative MCE (i.e., $\Delta S_M > 0$) is observed in the experimental data below 40 K, which becomes more positive with increasing field up to the maximum field of our apparatus (50 kOe). These results confirm the theoretical prediction of von Ranke *et al.*[8] of a negative MCE along the [111] direction. However, their model predicts that the negative MCE has a maximum (positive) value at 10 kOe ($\sim$2.7 J mol^{-1} K^{-1}) and $\sim$22 K, and then decreases with increasing field $\sim$2.2 J mol^{-1} K^{-1} at 20 kOe and 21 *K*, and $\sim$1.1 J mol^{-1} K^{-1} at 50 kOe and 19 K. In the mentioned theoretical work (Ref. 8), the authors used a mean field theory in Bak's framework[16] where the external field can be applied along any of the main crystallographic directions. This approach was an enhancement of the model published previously by some of us (Ref. 13) in which the external field could only be applied in a particular direction and it would agree satisfactorily with the experimental data obtained for polycrystalline $DyAl_2$. Besides the freedom to apply the external field in any crystallographic direction, the present model also includes a self-consistency for the free energy of the system. In other words, as we minimize the free energy for each temperature, the system is allowed to rotate from one direction to another. This procedure describes correctly our experimental data. It is seen that the experimental data show that MCE is about zero for $\Delta H = 10$ kOe and becomes more positive with increasing field to $\sim$1.8 J mol^{-1} K^{-1} for $\Delta H = 50$ kOe, and that the temperature of the negative MCE peak shifts rapidly with increasing field from $\sim$35 K for $\Delta H = 20$ kOe to $\sim$23 K for $\Delta H = 50$ kOe. Consequently, the positive ΔS_M peak is a direct result of the spin reorientation and the temperature of the peak's maximum value connected to the spin reorientation temperature, which decreases as the applied magnetic field increases.

Furthermore, as noted in the Theory section, the B_4 CEF parameter was changed by 0.4% from the value used by von

Ranke *et al.*, primarily to have better agreement between the observed and theoretical T_C (i.e., the T_C value derived from theory was increased by +3 K). As a result, there is excellent agreement between theory and experiment for the MCE along [111] direction in $DyAl_2$ [Fig. 8(b)].

The single-crystal values of the MCE are in good agreement with that reported for a bulk sample of $DyAl_2$ (Ref. 19). To compare the single crystal MCE values with that of the bulk polycrystal we calculated the weighed average values according to the multiplicity of the respective lattice directions. The single crystal bulk equivalent value for ΔS_M at 22 K for a 0–20 kOe field change was -0.3 J mol^{-1} K^{-1}, which is quite close to the actual bulk value of -0.25 J mol^{-1} K^{-1}; and at 60 K, the respective values were -2.0 and -1.9 J mol^{-1} K^{-1}. For a 0–50 kOe field change at 60 K, just below the MCE peak, the single crystal bulk equivalent ΔS_M was -3.9 J mol^{-1} K^{-1} compared to the actual bulk value of -3.7 J mol^{-1} K^{-1}.

Although the MCE values of many materials have been measured, especially over the past few years,[20–22] almost all of them have been polycrystals. Only a few single crystalline compounds [Tb_2PdSi_3 (Ref. 23)] and pure metals [Gd (Ref. 24) and Dy (Refs. 25 and 26)] have been studied in addition to the titled compound. All four materials exhibit anisotropic MCE values, which is not unexpected for the Tb_2PdSi_3, Gd, and Dy materials since all of them have a hexagonal crystal structure; however, $DyAl_2$ is cubic. The anisotropic ΔS_M values in the $DyAl_2$ compound are, as described above, due to crystalline electric field effects and the nonspherical $4f$ wave functions of the Dy component of $DyAl_2$

CONCLUSIONS

We performed a detailed study of five $DyAl_2$ single crystals, which were cut from the same large master single crystal and aligned along one of the three main crystallographic directions, by measuring the magnetization, susceptibility, and heat capacity. We conclude that this compound is anisotropic and its magnetic and magnetocaloric properties are direction dependent. A mean field theory was used in order to understand the experimental results, and, in general, there is good to fair agreement between theory and experiment. Furthermore, experiment confirms the predicted negative MCE along the [111] direction.

ACKNOWLEDGMENTS

The Ames Laboratory is operated by Iowa State University for the US Department of Energy (DOE) under Contract No. W-705-ENG-82. This research was supported by the Office of Basic Energy Sciences, Material Sciences Division of US DOE. One of us (A.L.L.) acknowledges the financial support from CNPq—Conselho Nacional de Desenvolvimento Científico e Tecnológico (Brazil).

*Present address: Los Alamos National Laboratory, MST-10, MS K764, Los Alamos, NM 87545, USA.

[1] V. K. Pecharsky and K. A. Gschneidner, Jr., Phys. Rev. Lett. **78**, 4494 (1997).
[2] V. K. Pecharsky and K. A. Gschneidner, Jr., Appl. Phys. Lett. **70**, 3299 (1997).
[3] F.-X. Hu, B.-G. Shen, J.-R. Sun, Z.-H. Cheng, G.-H. Rao, and X.-X. Zhang, Appl. Phys. Lett. **78**, 3675 (2001).
[4] S. Fujeida, A. Fujita, K. Fukamichi, Y. Yamazaki, and Y. Iijima, Appl. Phys. Lett. **79**, 653 (2001).
[5] W. Wada and Y. Tanabe, Appl. Phys. Lett. **79**, 3302 (2001).
[6] O. Tegus, E. Buck, K. H. J. Buschow, and F. R. de Boer, Nature (London) **415**, 150 (2002).
[7] K. A. Gschneidner, Jr. and V. K. Pecharsky, Annu. Rev. Mater. Sci. **30**, 387 (2000).
[8] P. J. von Ranke, I. G. de Oliveira, A. P. Guimaraes, and X. A da Silva, Phys. Rev. B **61**, 447 (2000).
[9] V. K. Pecharsky, K. A. Gschneidner, A. O. Pecharsky, and A. M. Tishin, Phys. Rev. B **64**, 144406 (2001).
[10] H.-G. Purwins and A. Leson, Adv. Phys. **39**, 309 (1990).
[11] V. K. Pecharsky, K. A. Gschneidner, and S. Malik, Adv. Cryog. Eng. **42**, 475 (1996).
[12] B. Barbara, M. F. Rossignol, H.-G. Purwins, and E. Walker, in *Crystal Field Effects in Metals and Alloys*, edited by A. Furrer (Plenum, New York, 1977), p. 148.
[13] P. J. von Ranke, V. K. Pecharsky, and K. A. Gschneidner, Jr., Phys. Rev. B **58**, 12110 (1998).
[14] E. M. Levin, V. K. Pecharsky, and K. A Gschneidner, Jr., J. Appl. Phys. **90**, 6255 (2001).
[15] K. R. Lea, M. J. Leask, and W. P. Wolf, J. Phys. Chem. Solids **23**, 1381 (1962).
[16] P. Bak, J. Phys. C **7**, 4097 (1974).
[17] V. K. Pecharsky and K. A. Gschneidner, Jr., J. Appl. Phys. **86**, 565 (1999).
[18] V. K. Pecharsky, J. O. Moorman, and K. A. Gschneidner, Jr., Rev. Sci. Instrum. **68**, 4196 (1997).
[19] V. K. Pecharsky and K. A. Gschneidner, Jr., Adv. Cryog. Eng. **42**, 423 (1996).
[20] K. A. Gschneidner, Jr. and V. K. Pecharsky, Annu. Rev. Mater. Sci. **30**, 387 (2000).
[21] K. A. Gschneidner, Jr. and V. K. Pecharsky, in *Intermetallic Compounds: Vol. 3, Principles and Practice*, edited by J. H. Westbrook and R. L. Fleischer (John Wiley & Sons, Ltd., New York, 2002), p. 519.
[22] K. A. Gschneidner, Jr., V. K. Pecharsky, and A. O. Tsokol, Rep. Prog. Phys. **68**, 1479 (2005).
[23] S. Majumdar, E. V. Sampathkumaran, P. L. Paulose, H. Bitterlich, W. Löser, and G. Behr, Phys. Rev. B **62**, 14207 (2000).
[24] S. Yu. Dan'kov, A. M. Tishin, V. K. Pecharsky, and K. A. Gschneidner, Jr., Phys. Rev. B **57**, 3478 (1998).
[25] A. S. Chernyshov, A. M. Tishin, K. A. Gschneidner, Jr., A. O. Pecharsky, V. K. Pecharsky, and T. Lograsso, Adv. Cryog. Eng. **48**, 19 (2002).
[26] A. S. Chernyshov, A. O. Pecharsky, A. M. Tishin, K. A. Gschneidner, Jr., and V. K. Pecharsky, Phys. Rev. B **71**, 184410 (2005).